Solid Freeform Fabrication 2017: Proceedings of the 28th Annual International Solid Freeform Fabrication Symposium – An Additive Manufacturing Conference
Reviewed Paper

Fatigue behavior of additive manufactured parts in different process chains – An experimental study

Eckart Uhlmann[a], Georg Gerlitzky[a], Claudia Fleck[b]

[a]Institute for Machine Tools and Factory Management (IWF), TU Berlin, Pascalstraße 8-9, Berlin, Germany
[b]Department of Materials Engineering, TU Berlin, Straße des 17. Juni 135, Berlin, Germany

Abstract

Metal based Additive Manufacturing (AM) has experienced dynamic growth in recent years. However, the global distribution of Additive Manufacturing is limited by the fact the produced parts suffer from bad surface quality and the material properties concerning fatigue life are still an object of current investigations which limits possible applications of AM parts. Due to this fact metal AM processes are often followed by a post process to ensure a better surface quality. In this paper the authors present results where fatigue life and different post processes of additive manufactured parts are investigated. Subsequently, surface roughness, high cycle fatigue, fracture behavior and microstructure have been characterized. Finally the results for the different post processing states have been compared and surface properties as well as microstructure have been correlated with the fatigue properties in order to evaluate how different process chains influence the High cycle fatigue (HCF) behavior of additive manufactured parts.

Introduction

Freeform fabrication processes such as Selective Laser Melting (SLM) offer high geometrical freedom compared to conventional manufacturing processes like turning milling or grinding. In addition the relevance of Selective Laser Melting is steadily growing as it applicable to a wide range of materials and it empowers the fast production of prototypes and serial components.
Therefore, Selective Laser Melting delivers an answer to the continuously increasing complexity of serial components and enables the resource saving manufacturing of complex parts and hard to machine components [1]. Especially in the aviation industry SLM is already successfully adapted for serial components due to the expensive materials used and the high material removal of conventional manufacturing processes. At the moment however SLM is only cost efficient in certain business cases and is preferred at low production volumes, high raw material costs and at the processing of hard to machine materials. This is mainly due to the fact that the fixed costs of the SLM process are lower than the fixed costs of comparable conventional manufacturing processes while the recurring costs of the SLM processes are higher than conventional manufacturing processes [2].
Currently the main problems concerning Additive Manufacturing processes are the achievable surface quality, geometrical accuracy, uncertainty about mechanical properties and high costs [3]. Due to these problems SLM manufactured parts often need to be post processed with manufacturing processes such as turning, milling, blasting or vibratory finishing. In this paper the authors present a work which unites different post processes and fatigue life of additive manufactured parts. First, parts are produced with Selective Laser Melting with constant process parameters such as laser power or scanning speed. After this the parts are post processed with

vibratory finishing and turning followed by an investigation concerning roughness, high cycle fatigue (HCF) and fracture behavior. Finally the results for the different post processing states have been compared and surface properties and microstructure have been correlated with the fatigue properties in order to evaluate how different process chains influence the HCF behavior of additive manufactured parts.

Experimental Setup

All parts were produced on the SLM machine SLM 250 HL, MTT Technologies GmbH, Lübeck, located at the Production Technology Center in Berlin, Germany. To process the specimens stainless steel powder 316L (1.4404) was used with a typical grain size distribution of 20 to 63µm. The powder properties were obtained from the suppliers' certificate following European standard DIN EN 10204. The chemical composition of the powder is given in Table 1. A scanning electron microscopy (SEM) image of the powder is shown in Figure 1.

Table 1: Chemical composition of processed powder

Element	Fe	C	Si	Mn	Cr	Mo	Ni
Mass percentage	Bal.	0.02	0.8	1.7	17.7	2.2	10.5

The image illustrates that not all powder particles have a spherical form which might result in a lower flowabilty of the powder. Due to the fact that stainless steel powder normally offers high flowabilty rates the shown powder sizes should also offer an acceptable flowability rate. This assumption was validated with Hall-flowability measurements which showed an average flow time of 3.4 s.

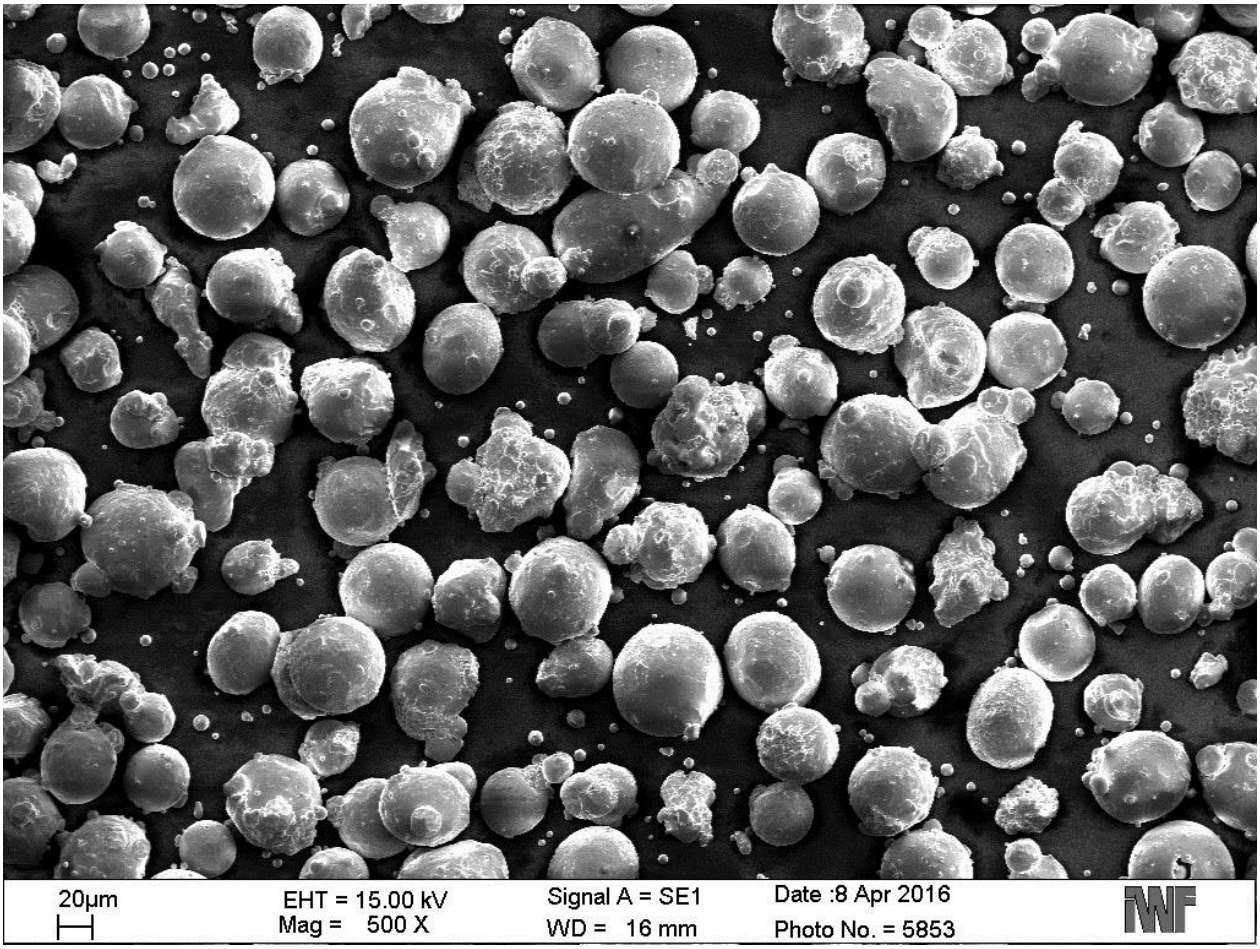

Figure 1: SEM image of processed stainless steel powder

The parts were produced with optimized building parameters regarding density of the part and process time, provided by the machine supplier and are shown in table 2. These parameters are commonly used for the SLM process and are therefore used as reference parameters for the different process chains. All specimens were oriented vertically on the building platform.

Table 2: Overview of SLM process parameters

Process parameters	
Layer thickness	0.05mm
Laser power	275 W
Scanning speed	760 mm/s
Hatch pattern	Chess
Hatch distance	0.12mm

Test specimen

Two different specimen geometries were produced for the different post processes. Specimen A was used for the turning process. It is clearly visible that this specimen significantly differs from specimen B which was used for the vibratory finishing process and the SLM shape HCF

investigations. This is mainly due to the fact that the part has to be longer in order to be clamped inside the machine tool. The dimensions are illustrated in Figure 3.

Specimen A was produced with SLM and post processed with turning which lead to specimen D (figure 2). The building direction is indicated with a black arrow. Specimen B was produced with SLM with no further post process. Specimen C was produced with SLM followed by an additional vibratory finishing process.

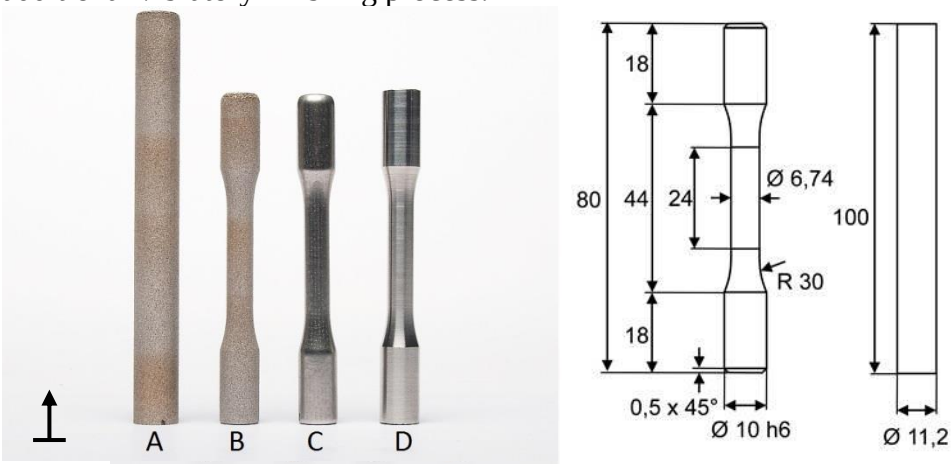

Figure 2: Dimensions and illustration of different specimens

The post processes were selected because they are commonly used as post processes for SLM parts in industry and research. Especially vibratory finishing could be a promising finishing process for SLM parts because the accessibility of geometrical complex structures of SLM parts is possible due to the small abrasive media used. The turning process was carried out on a CTX gamma 1250 CT machine from DMG Mori Europe Holding AG, Winterthur, Switzerland. The vibratory finishing process was carried out as a two stage process on a MF 8/1, Multi finish GmbH & Co. KG, Schömberg. In a first process step triangular abrasive media was used for a process time of 120 minutes. In a second process step cylindrical abrasive media was used for a process time of 60 minutes. The process parameters for the turning and the vibratory finishing process are given in table 3 and table 4.

Table 3: Process parameters of the turning process

Turning process	
Depth of cut a_e	0.5 mm
Feed f	0.15 mm/ rev.
Cutting speed v_c	140 m/min

Table 4: Process parameters of the vibratory finishing process

Vibratory finishing process	1st process step	2nd process step
Processing time	120 min	60 min
Abrasive media	Triangular	Cylindrical
Excitation frequency f_e	50 Hz	50 Hz

Microstructural investigations
For the microstructural characterization, longitudinal and cross-sections for each kind of specimen were prepared. The longitudinal sections contain the area of the fracture origin and the final fracture; the cross-sections are situated about 1 cm below the fracture surface. After grinding and polishing, the sections were etched with V2A-etchant to develop the microstructure

Roughness measurements
All surface roughness measurements were conducted with the tactile measurement system Hommel Nanoscan etamic 855, Jenoptik, Jena. The investigated target values were Ra and Rz. All specimens were measured three times and turned by 120 degrees to ensure reproducibility for all measurements. The average value of these three measurements was taken to obtain the target value of one specimen. In addition, the mean standard deviation was calculated for all measurements.

High cycle fatigue (HCF) test series
High cycle fatigue tests were performed with a rotating bending machine (Carl Schenck AG, Darmstadt, type Rapid *Punz*) at a frequency of 100 Hz under air cooling to a maximum number of cycles (N_{max}) of 10^7. Two surface stress amplitudes were chosen in the HCF range for each finishing state to yield numbers of cycles to failure (N_f) of about 5^x10^5 and 2^x10^6. Further specimens were tested at lower surface stress amplitudes, in the transition range to the endurance limit.

SEM analysis
The fracture surfaces of selected specimens, all tested with surface stress amplitudes leading to failure within 10^6 cycles, were investigated by scanning electron microscopy (SEM; CamScan REM Serie 2, Obducat, Lund, Sweden) at an accelerating voltage of 20 kV in the secondary electron mode. The specimens were cut about 1 cm below one of the fracture surfaces under continuous water-cooling while the fracture surfaces were protected by a polymer cover, and imaging was performed after ultrasonic cleaning in ethanol.

Comparison with state of the art fatigue testing
Fatigue testing of additive manufactured products has already been investigated by some researchers e.g. [4], [5], [6]. The main testing method was the four point bending test as in this work. Often the main focus was to compare different heat treatment strategies or build orientations to ensure the best possible fatigue life [5], [6]. In some works even a concrete product was produced with AM and successfully dimensioned in terms of fatigue life [4]. In other work the focus was to develop the best possible process parameters for the highest possible fatigue life [7].
The results in this work correlate well with other works regarding the dependency of roughness and fatigue life. A unique feature of this work is to reveal the differences between the examined process chains regarding fatigue life as well as different fracture behaviors. This should be helpful to identify reasonable holistic process chains for AM.
Initially 60 specimens were produced with SLM followed by the different post processes turning and vibratory finishing. In total 20 of each kind of specimens (B, C and D) were produced. Subsequently, for all specimens the surface roughness was determined. The microstructure and the fracture behavior of one typical specimen of each kind was investigated by light and scanning

electron microscopy (LM, SEM), respectively. After this, all specimens were tested regarding their high cycle fatigue behavior on the Punz machine.

Results/ Discussion

Microstructural investigations

Figure 3 shows the typical microstructure of the SLM manufactured specimens. The building direction is indicated with an arrow, in this case perpendicular to the image plane. It consists of an austenitic microstructure. The cross-sections also nicely represent the hatch pattern of the manufacturing process. Each of the longitudinal structures is made up of many grains which lack the polygonal structure usually observed in austenitic steels. In some areas, dendrites are visible. All specimens contain binding defects, visible as black voids.

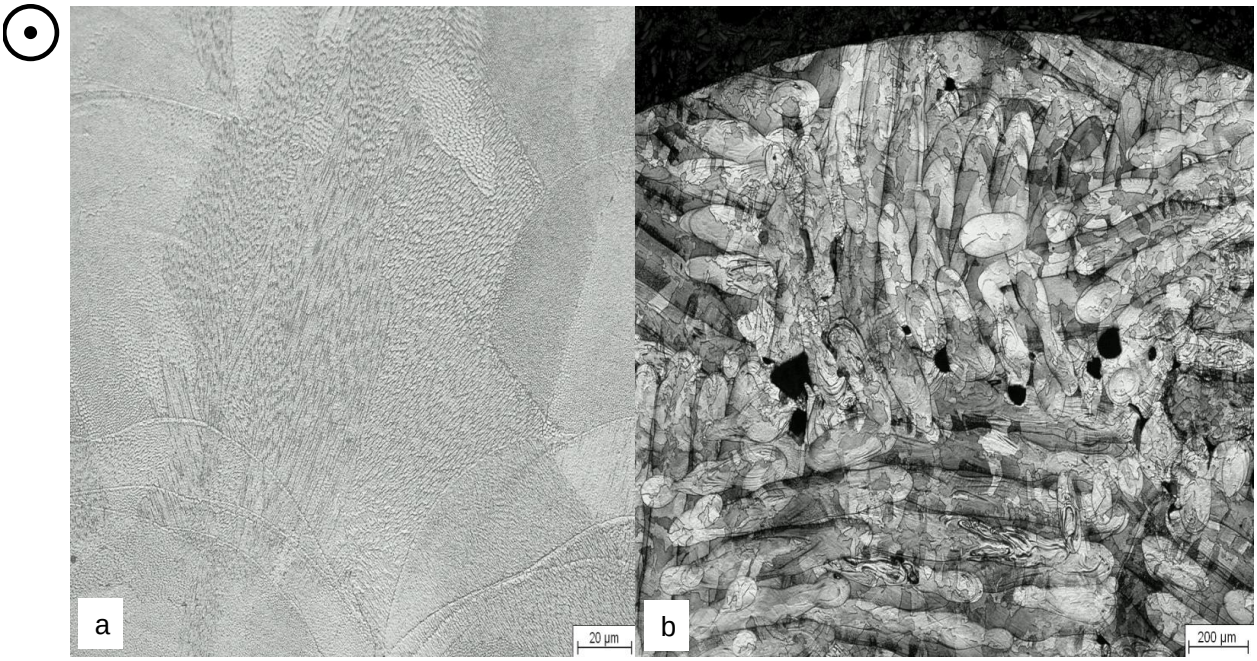

Figure 3: (a) Austenitic microstructure; (b) Scanning pattern of a turned specimen

The surface of the turned specimen is smooth with some voids present. The surface of the vibratory finished specimen is also very smooth, and the microstructure just below the surface looks plastically deformed. Nevertheless, more shallow defects are visible on the surface than on the turned surface. The SLM shape specimen has a very rough surface. Numerous large defects and molten and re-solidified powder particles are visible and indicated with white arrows in figure 4(b).

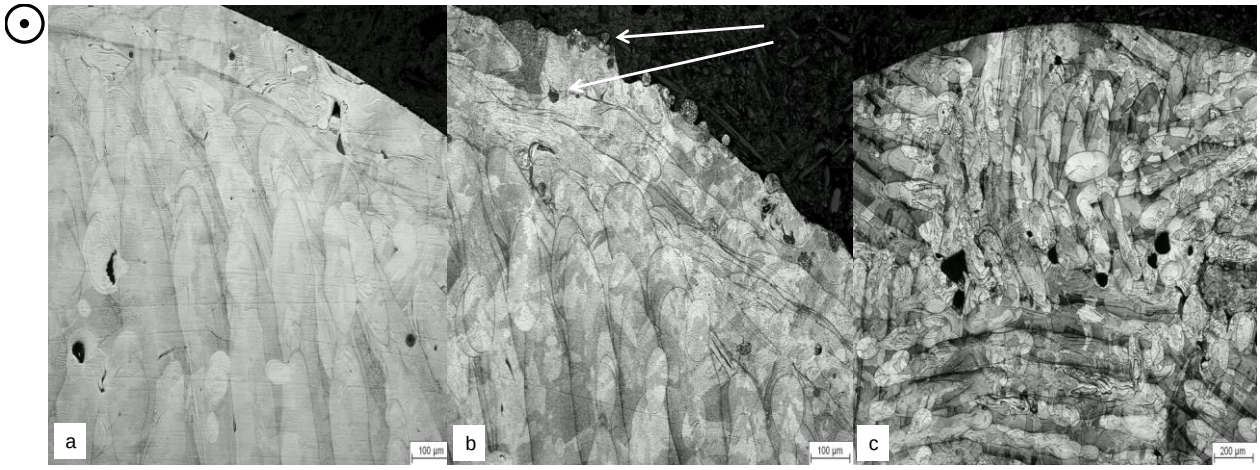

Figure 4: Comparison of differently post processed surfaces (a) Vibratory finished (b) SLM-near net shape (c) Turned

The longitudinal section in figure 5 a2 shows a secondary crack that runs through a binding defect just below the surface. We may assume that this fatigue crack originated at this defect but could not develop into a dominant crack due to higher crack growth in the level of the later fracture surface. Nevertheless, more shallow defects are visible on the surface than on the turned surface.

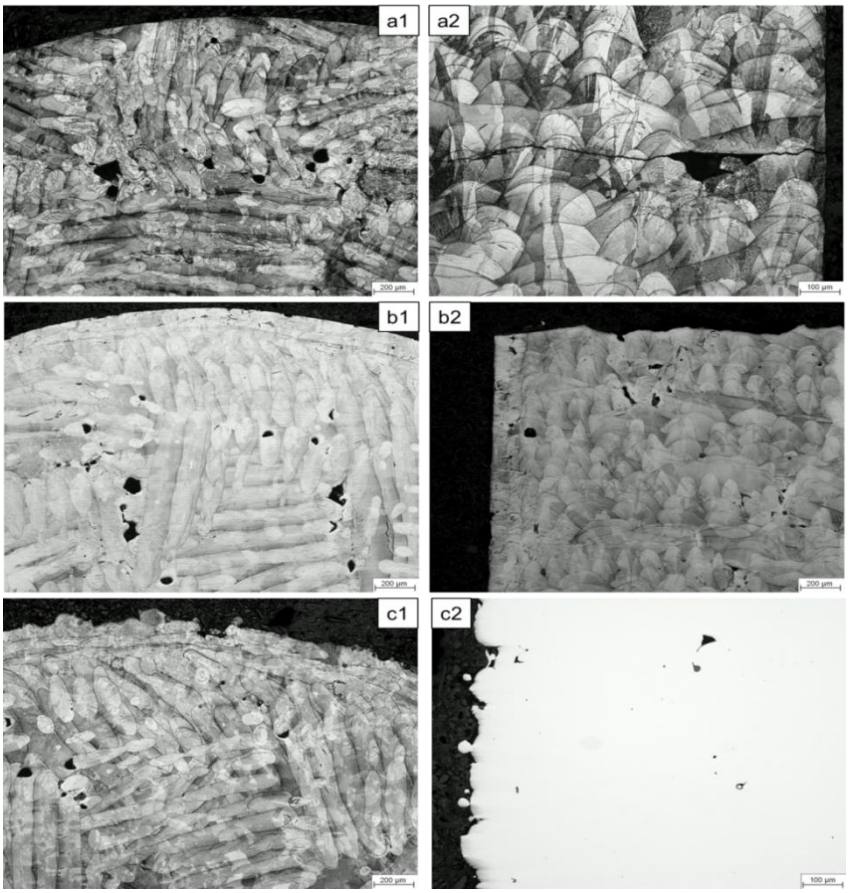

Figure 5: LM: cross-sections (left row, "1") and longitudinal sections (right row, "2") of a) turned, b) vibratory finishing, c) SLM shape specimens. Note the different scale of b2 as compared to a2 and c2.

Roughness measurements

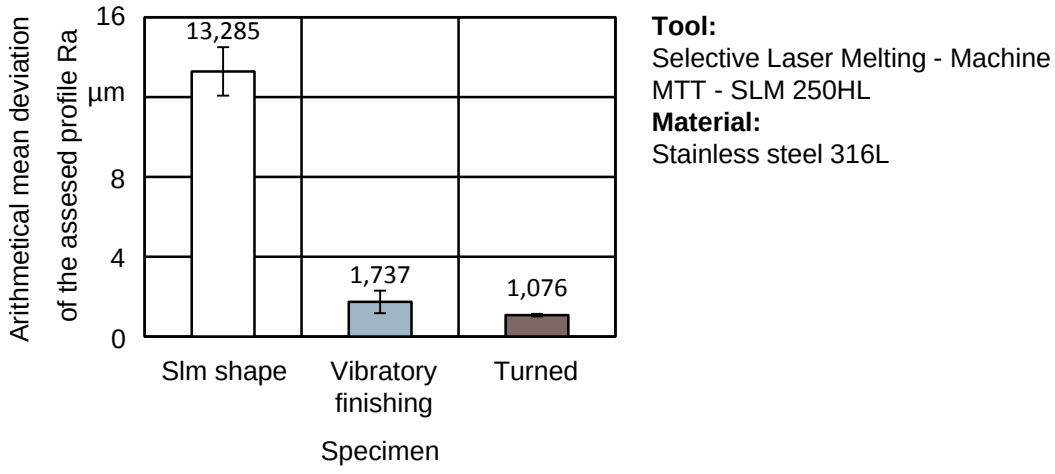

Figure 6: Arithmetical mean deviation of the assessed profile Ra of specimens

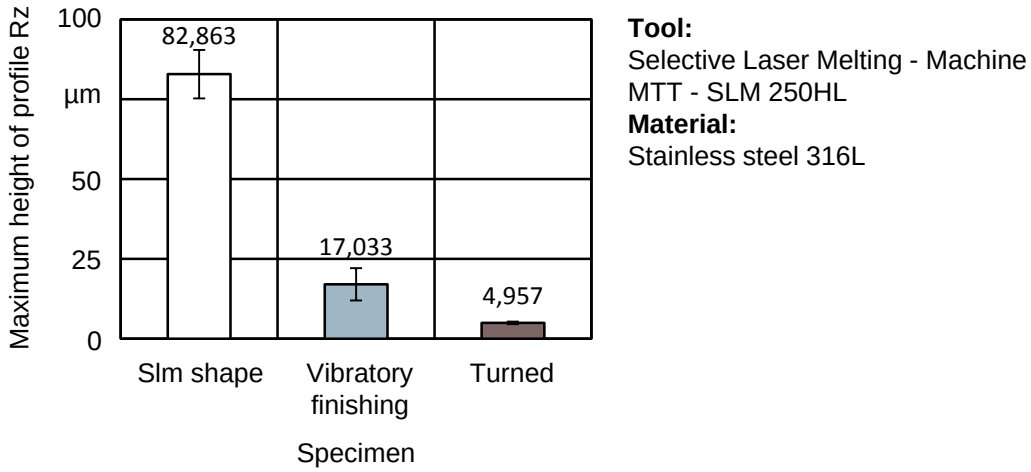

Figure 7: Maximum height of profile Rz of specimens

Figure 6 and Figure 7 show the measured target values Ra and Rz for the different specimens. The SLM shape specimens have by far the highest surface roughness of all specimens with a roughness Ra of 13.29 and Rz = 82.86. The vibratory finished specimens have a mean arithmetic surface roughness of Ra = 1.74 and Rz = 17.03. Turned specimens showed the best surface roughness with Ra of 1.08 and Rz 4.96. The vibratory finished specimens have a significantly higher surface roughness than the turned specimen for both target values Ra and Rz. Better surface qualities for the vibratory finishing process could be obtained with a longer process time and special abrasive media, due to the fact that fatigue resistance is highly dependent on the surface roughness [8]. This may lead to a low fatigue resistance of the SLM shaped specimen, with the turned specimen possibly showing the best fatigue resistance. The measurements also revealed the highest standard deviation for SLM shape specimen. The high surface roughness is mainly due to the fact that the typical particle size distribution for the SLM process is 20 to 63 µm. This limits the achievable surface quality. With a smaller particle size distribution better surface qualities would be achievable but this contains other risks and problems such as respirability of the finer powder and worse flowability of the powder. The higher standard deviation has two possible reasons. First, the poor reproducibility of SLM manufactured parts, because of different temperatures in the melt pool which are caused by a non-symmetrical protective gas flow and the location of the part on the building platform during the process which causes different heat transfer coefficients. The second reason is the measurement systems. Due to the high surface roughness optical as well as tactile measurement systems reach their limits [9]. Optical measurement systems struggle with reflecting surfaces while the stylus tip of a tactile measurement can break due to possible undercuts and pores of the selective laser melted part.

High cycle fatigue (HCF) test series

Figure 8 illustrates typical striation due to the cyclic loading while Figure 9 shows the results of the rotating bending tests. The dashed lines in the HCF regime are a guide for the eye to highlight the fatigue life ranges of the differently finished SLM specimens. The gray arrows denote specimens that did not fail at cycle numbers above the defined maximum number of cycles to failure (N_{max}, denoted by the bold black line). The SLM shape specimens exhibit the lowest fatigue life resistance.

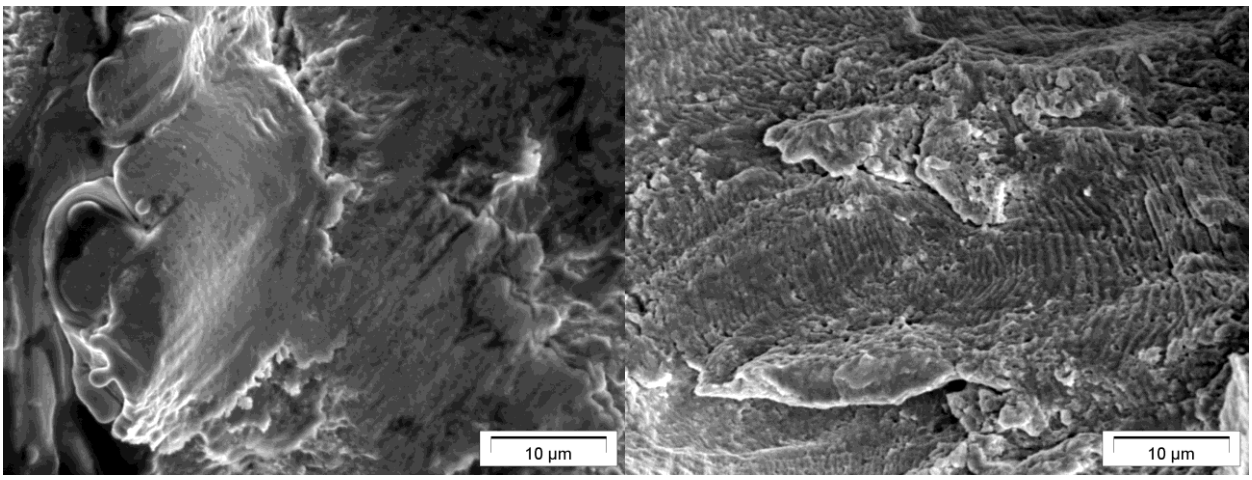

Figure 8: Striation of HCF specimens

After vibratory finishing or turning, the life expectancy increases clearly. The differences seem to be slightly higher for higher surface stress amplitudes, and slightly lower for stress amplitudes in the transition range. The SLM shape and vibratory finished specimens show a huge scatter in the fatigue life, specifically in the transition range, with specimens failing at around $N_f = 2^x10^6$ while others survive $N_f = 2^x10^7$ at the same surface stress amplitude. For the turned specimen, the numbers of cycles to failure scatter much less in this fatigue range. The results of the fatigue tests correlate well with the differences in surface roughness between the specimen types. Local height variations on the surface originating from the powder particle size, as in the SLM shape specimens, or from turning marks as in the turned specimens, act as stress raisers. Fatigue failures usually originate from the surface; furthermore, in rotating bending tests the highest tensile stresses act at the surface. Rougher surface states result in locally even higher stresses, corresponding with lower numbers of cycles to failure. The higher fatigue endurance of the vibratory finished and turned specimens may further be due to compressive residual stresses originating from the finishing procedures. Further, defects just below the surface might be compressed by plastic deformation near the surface. Especially in [5] the same material was tested with the same testing method and the same orientation on the building platform. The results correlate as the specimen failed between 10^6 and 10^7cycles and a maximum stress at knee point of 180 MPa for as built specimens. In that paper also a significant increase through machining the specimens was observed. However results may differ due to the fact that a different SLM machine and different machining techniques were used. In addition it is hard to compare different investigations regarding fatigue because different materials, surface integrity and SLM machines are investigated.

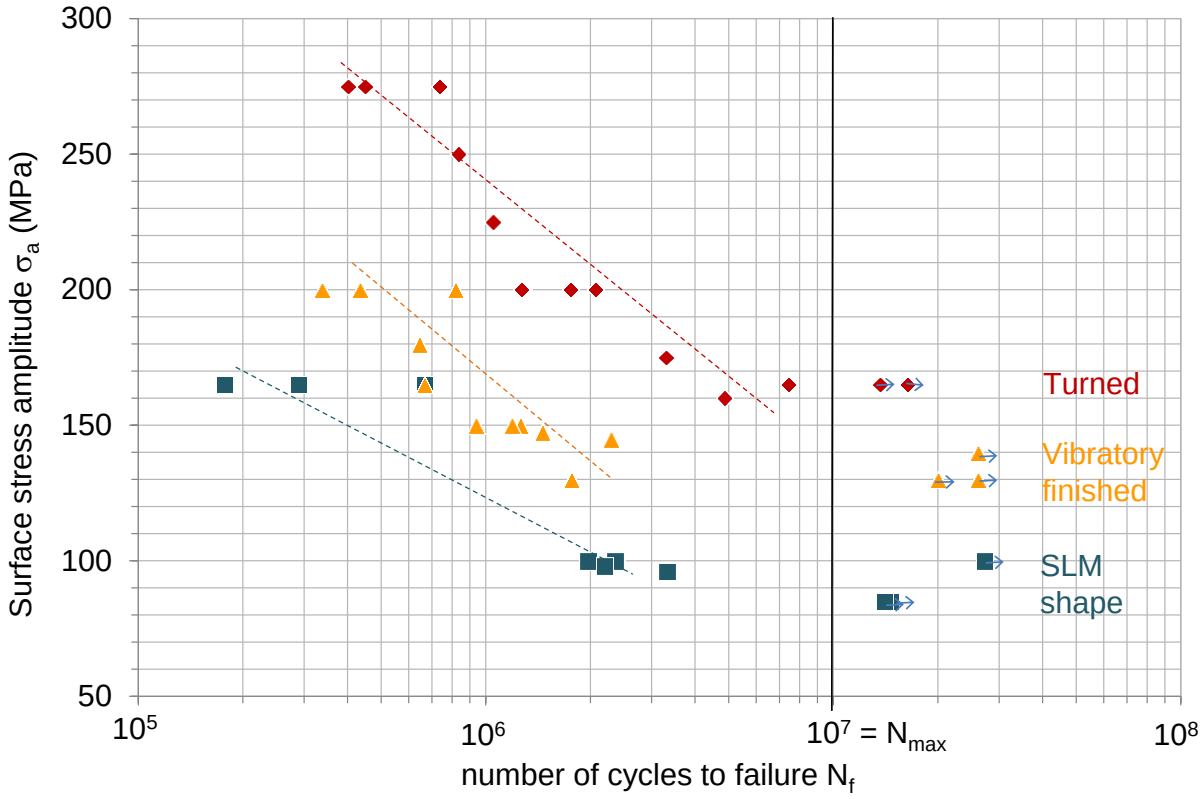

Figure 9: S, N-curves for SLM-316L specimens

SEM analysis

Typical fracture surfaces of specimens that failed at about 10^6 cycles are shown in Figure 10. The surveys in the upper row show the smoother fatigue and rough final fracture areas. All specimens exhibit several failure origins, denoted by arrows: The continuous arrows with a bold head point to the one (a1, b1) or two (c1) main, dominant fracture origin(s), and the dashed arrows with a line-head point to additional non-dominant origins. The higher magnification micrographs in the bottom row show the area of the dominant, or of one of the dominant fatigue origins on the fracture surfaces together with the specimen surfaces nearby. All fatigue failure(s) originated at binding defects at (a2, b2) or just below (c2) the surface. Please note that the magnified sections of the vibratory finished and the turned specimen are oriented in the same direction as the survey above while the SLM shape specimen has been rotated clock-wise by 90° to acquire the magnified view.

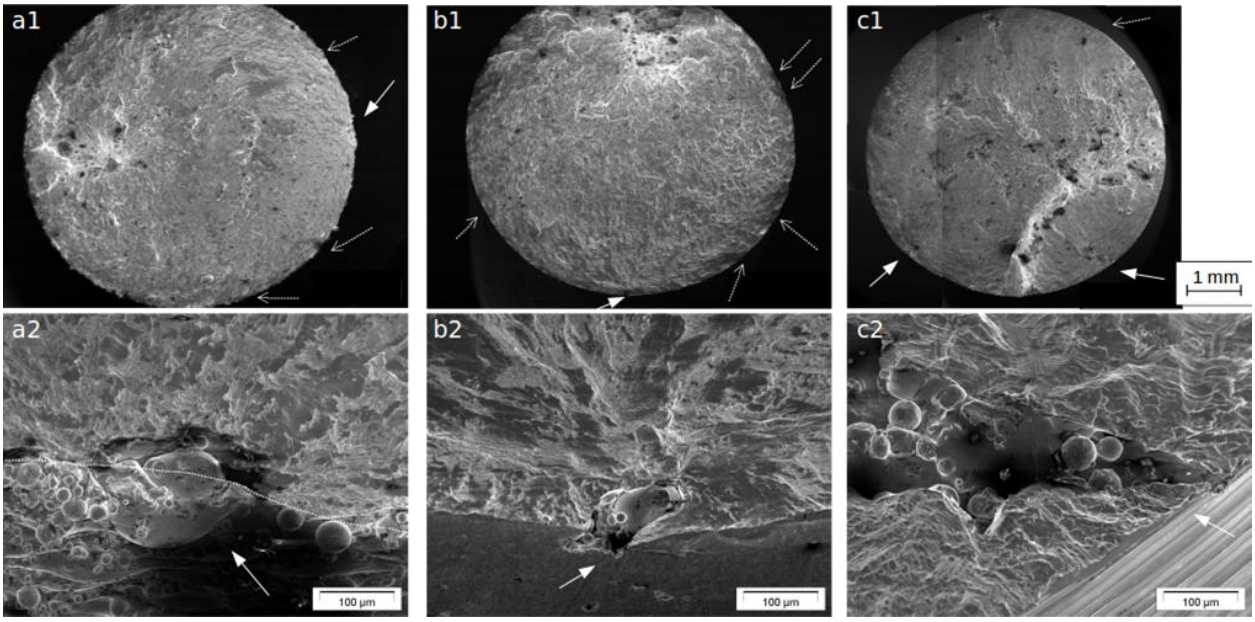

Figure 10: SEM micrographs of fracture surfaces of specimens with different surface finishing: a) turned, b) vibratory finishing, c) SLM shape; all loaded with surface stress amplitudes leading to numbers of cycles to failure in the range of $N_f = 10^6$

While the SLM shape specimens exhibit a rough surface, with rounded powder particles clearly visible (a2; the white dashed line serves as a guide to the eye to discriminate the fracture and specimen surfaces above and below the line), the vibratory finished specimens have a relatively even and smooth surface (b2). Turning marks are visible on the surfaces of the turned specimens (c2). Inner defects just below the surface act as local stress raisers; together with the different surface roughness features and possible compressive residual stresses in the surface finished states, they define the local stress state, and failure starts where the local tensile stresses are highest (comp. figure 9a2).

The final fracture surfaces show dimples, as to be expected for the inherently ductile austenitic materials, and occasional fatigue striations were observed on the fatigue fracture surfaces (data not shown). The black areas on the micrographs are due to charging effects of only partially attached or less electron-conductive particles on the surfaces and fracture surfaces, usually found within depressions.

Conclusion

In this work the influence of two different post processes for Selective Laser Melted specimens regarding their fatigue behavior was investigated. The investigated material was stainless steel 316L. The approach showed that the bad surface quality of additive manufactured parts is a key problem of this technology, not only for functional surfaces, but as well for the fatigue life. Turned specimens showed the best fatigue behavior while SLM manufactured specimens showed the worst. This correlates well with the obtained surface roughness, also the data for fatigue life of SLM manufactured and vibratory finished specimens scatter a lot. However the results also showed that even though overall a high material density exists, small

defects such as unmolten powder particles lead to dominant cracks. These results demonstrate the importance of integrating the SLM process into an appropriate and cost efficient process chain to increase the fatigue life of additive manufactured parts and spread the applications possibilities of SLM. In the future hard to machine materials, produced by SLM, such as titanium or nickel based alloys which are used for dynamically loaded operations in aviation should be investigated regarding different process chains. In addition the conventional process chain should be compared with the additive manufacturing process chain regarding fatigue life of the produced parts. Concluding, other process chains such as blasting should be investigated and these results should be combined with existing results regarding heat treatment methods.

References

[1] Meiners, W. Direktes Selektives Laser Sintern einkomponentiger metallischer Werkstoffe, Dissertation, Shaker Verlag, Aachen, 1999.

[2] W. Frazier. Metal Additive Manufacturing: A review. Journal of Materials Engineering and performance, Vol 23 ,6, 1917-1928, 2014.

[3] E. Yasa, J-P. Kruth, J. Deckers. Manufacturing by combining Selective Laser Melting and Selective Laser Erosion/laser re-melting. CIRP Annals- Manufacturing Technology, 263-266, 2011.

[4] Stoffregen, H., Butterweck, K., Abele, E., Fatigue analysis in selective laser melting: Review and investigation of thin- walled actuator housings, 25th Solid Freeform fabrication symposium, Austin, Texas, 2014.

[5] Spierings, A. B., Starr, T. L., Wegener, K. Fatigue performance of additive manufactured metallic parts, Rapid Prototyping Journal, Vol 19 (2), 88-94, 2013.

[6] Sehrt, J.T. Witt, G. Dynamic strength and fracture toughness analysis of beam melted parts. Proceedings of the 36th International MATADOR conference, 385-388, 2010.

[7] Van Hooreweder B., Boonen R., Moens D., Kruth J., Sas P. (2012). On the determination of fatigue properties of Ti6Al4V produced by selective laser melting. In Russell, S. (Ed.), Structures, structural dynamics, and materials and co-located conferences 53rd aiaa/asme/asce/ahs/asc. AIAA Structures, Structural Dynamics and Materials Conference. Honolulu, Hawaii, USA, 23-26 April 2012. Reston, VA: American Institute of Aeronautics and Astronautics.

[8] E. Uhlmann, P. John, V. Kashevko, G. Gerlitzky, A. Bergmann. Quality optimized Additive Manufacturing through Measuring System Analysis. Proceedings, ASPE Spring topical meeting, 83-88, 2015.

[9] M. Suraratchai, J. Limido, C. Mabru, R. Chieragatti. Modelling the influence of machined surface roughness on the fatigue life of aluminum alloy. International Journal of fatigue, Vol 30, 12, 2119-2126.